SPE-199741-MS

Utilizing Discrete Fracture Modeling and Microproppant to Predict and Sustain Production Improvements in Micro Darcy Rock

Carl T. Montgomery, Michael B. Smith, and Zhongfeng An, NSI Technologies L.L.C.; Hank H. Klein, HK Technologies; William Strobel, Zeeospheres Ceramics Inc; Roger R. Myers, RRM Completions, LLC.

This paper was prepared for presentation at the SPE Hydraulic Fracturing Technology Conference and Exhibition held in The Woodlands, Texas, USA, 4-6 February 2020.

Abstract

Providing and sustaining fracture conductivity in secondary fracture systems created during the stimulation of very tight unconventional shale plays is critical for sustaining productivity and reducing decline rates. In this paper, a discrete fracture network model which includes proppant transport will be utilized to show the effect that an unsupported vs supported dilated fracture network has on the decline and ultimate recovery of available resources in shale. In addition, the characteristics and properties of a microproppant will be described. The physical properties of the material, the oil and water conductivity of the proppant at various fracture widths along with the resultant Fcd will be presented. Utilizing a bridging factor of 3, a comparison of the surface area propped by various proppants will be made. The proppant transport characteristics will also be described. The production benefits of utilizing very small proppants will be demonstrated utilizing production data from four different rock systems including the Barnett, Woodford, Utica, Permian Basin and Marcellus shale. Several additional operational benefits including reduced pumping pressures and far field diversion to prevent fracture hits will also be discussed. Finally, operational considerations will be described including utilizing liquid slurry's, pump wear evaluations and recommended proppant addition points will be described.

Introduction

The difference between the hydraulically created and productive propped fracture area in the very low permeability unconventional shale plays currently being stimulated can be significant. As Figure 1 shows, when a well is fractured the unpropped fracture in the native rock will have some natural permeability created by the asperities or roughness on the rock surface. As the rock is subjected to increases in effective stress, the nature fissure permeability will be lost. This loss in the natural flow capacity of the fracture happens for two basic reasons. The first is because of the effective stress on the rock. The initial effective stress increases as the well is produced because of a drop in the reservoir pressure.

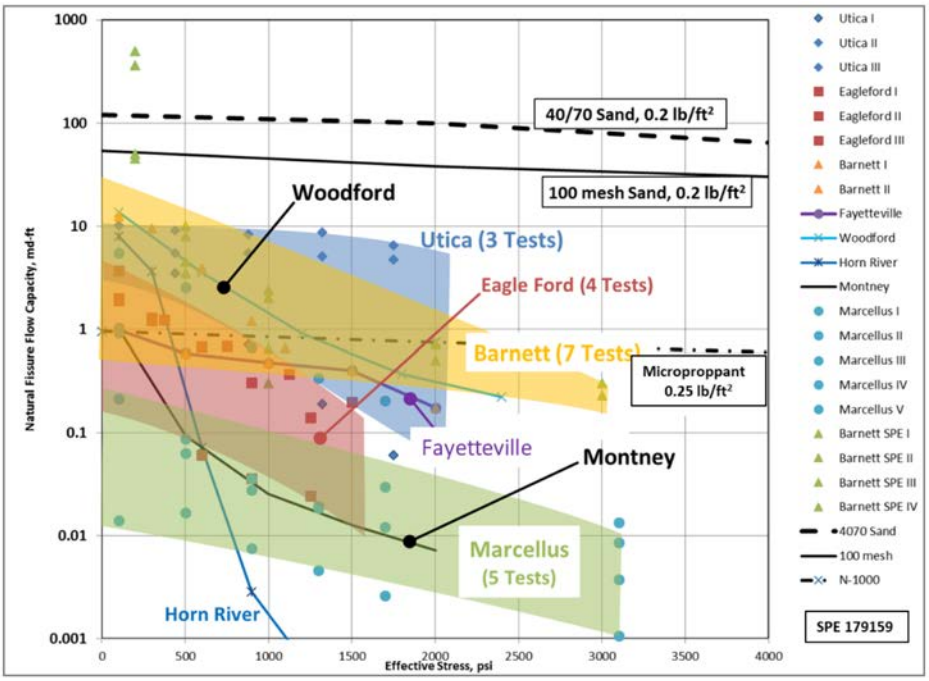

Figure 1—Natural Fissure Permeability vs Effective Stress for various shale plays

Secondly, as Figure 2 from Sone and Zoback two-part series on the Mechanical Properties of Shale-Gas Reservoir Rocks shows, when the rock is subjected to stress, the rock will creep with time.

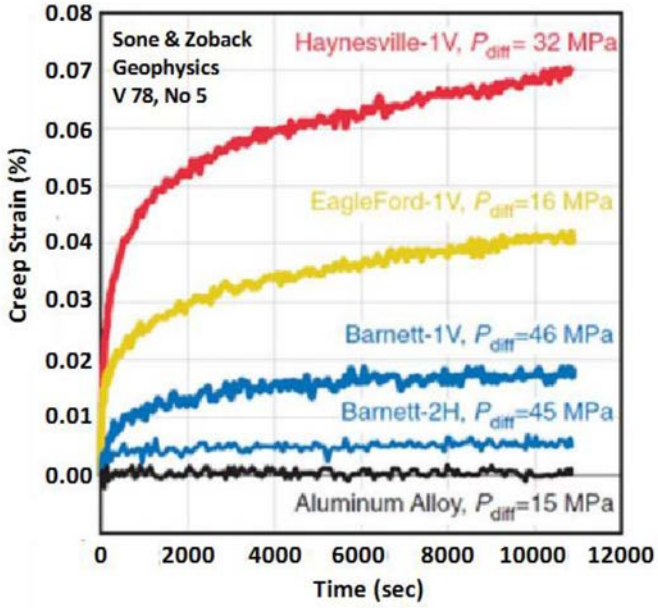

Figure 2—Rock Creep Under Load for three shale types

To counteract this natural loss in permeability, proppants are added to the fracturing fluid to support and maintain the flow capacity of the fracture. Table 1 shows a typical pump schedule used to fracture a shale well. As the schedule shows, the formation and perforations are first cleaned up with acid followed by a pad to initiate the fracture. To prop the fracture, two different sizes proppants, 70/140 or 100 mesh and 40/70 mesh, are added to the slickwater fracturing fluid. Some operators only pump 100 mesh sand and

most of the sand used comes from local sources located near the operator's fields. The schedule is pumped as a single stage into typically 6 to 8 perforation clusters spaced along the horizontal wellbore. The general rule for a proppant to enter a fracture says that the fracture width must be 3 times the mean particle size trying to enter a fracture [12,13].

Table 1—Typical shale well treatment schedule

Treatment Schedule												
Stage Type	Slurry Rate (BPM)	Clean Volume (Gal)	Clean Volume (Bbls)	Cum Clean Volume (Bbls)	Slurry Volume (Gal)	Slurry Volume (Bbls)	Cum Slurry Volume (Bbls)	Prop Concentration (ppg)	Proppant Type	Proppant Stage (Lbs)	Cum Proppant (Lbs)	Pump Time (Min)
Slickwater Break Down	15	1050	25	25	1050	25	25	0.00		0	0	1.7
7.5% HCl	15	1500	36	61	1500	36	61	0.00		0	0	2.4
Slickwater Spacer	20	2100	50	111	2100	50	111	0.00		0		2.5
7.5% HCl	15	1500	36	146	1500	36	146	0.00		0		2.4
Slickwater Pad	90	36000	857	1004	36000	857	1004	0.00		0		9.5
Slickwater w 0.25 ppa	90	20000	476	1480	20227	482	1485	0.25	70/140 Mesh Sand	5000	5000	5.4
Slickwater w 0.5 ppa	90	20000	476	1956	20453	487	1972	0.50	70/140 Mesh Sand	10000	15000	5.4
Slickwater w 1.0 ppa	90	20000	476	2432	20906	498	2470	1.00	70/140 Mesh Sand	20000	35000	5.5
Slickwater w 1.5 ppa	90	20000	476	2908	21359	509	2978	1.50	70/140 Mesh Sand	30000	65000	5.7
Slickwater w 2.0 ppa	90	20000	476	3385	21812	519	3498	2.00	70/140 Mesh Sand	40000	105000	5.8
Slickwater w 2.25 ppa	90	10000	238	3623	11019	262	3760	2.25	70/140 Mesh Sand	22500	127500	2.9
Slickwater w 0.5 ppa	90	18000	429	4051	18408	438	4198	0.50	40/70 Mesh Sand	9000	136500	4.9
Slickwater w 1.0 ppa	90	30000	714	4765	31359	747	4945	1.00	40/70 Mesh Sand	30000	166500	8.3
Slickwater w 1.5 ppa	90	30000	714	5480	32039	763	5708	1.50	40/70 Mesh Sand	45000	211500	8.5
Slickwater w 2.0 ppa	90	30000	714	6194	32718	779	6487	2.00	40/70 Mesh Sand	60000	271500	8.7
Slickwater w 2.25 ppa	90	60000	1429	7623	66116	1574	8061	2.25	40/70 Mesh Sand	135000	406500	17.5
Flush	90	15000	357	7980		357	8418	0.00				4.0
Totals		335150	7980			8418				406500		100.8
									Volume Factor for Sand =	0.0453		

Using this criteria, Table 2 outlines the fracture aperture required to accept various proppant sizes. For example, if 100 mesh sand is used to prop the fracture the hydraulic fracture width needs to be wider than a half millimeter or 0.02 inches to accept the proppant. Laboratory work by Kim et.al.[8] using split shale core plugs from EagleFord, Bakken and Barnett formations show that even a monolayer of microproppant will dramatically increase the conductivity of a unpropped fractured core.

The portion of the fracture that is created by the fluid is termed the "Hydraulic Fracture Area", whereas the area able to accept proppant is termed the "Propped Fracture Area". As described in the following sections, this can lead to a substantial portion to the fracture unpropped. Because this unpropped area has some natural flow capacity that diminishes with time, as described earlier, the wells will have production rates that rapidly decline over time because of the loss of the natural flow capacity of the rock. The long-term production is provided by the "Propped Fracture Area" of the rock.

Table 2—Bridging size for various proppants (*Particle size measured by laser diffraction using a Mastersizer 2000)

Proppant	D90 Size in Microns*	Bridging Factor	Fracture Aperture (mm)	Fracture Aperture (inches)
20/40	825	3	2.475	0.097
40/70	502	3	1.506	0.059
100 Mesh	303	3	0.909	0.036
Microproppant	70	3	0.210	0.008

As Figure 3 shows, the production decline for shale wells is very steep with 60 to 70 percent of the initial production being lost in the first year. Typically, this steep decline will continue for a couple of years then the wells will go on a steady-state decline for many years. Much of this early decline is caused by depletion

of the natural fracture network and at least some of the decline is due to loss of the natural flow capacity of the stimulated fracture network. By introducing a very small proppant into the very narrow stimulated fracture system thus giving long term conductivity, the decline curve should flatten with reserves being recovered earlier. The following sections describe how this can be modeled and what the effect is on the production decline in several shale plays.

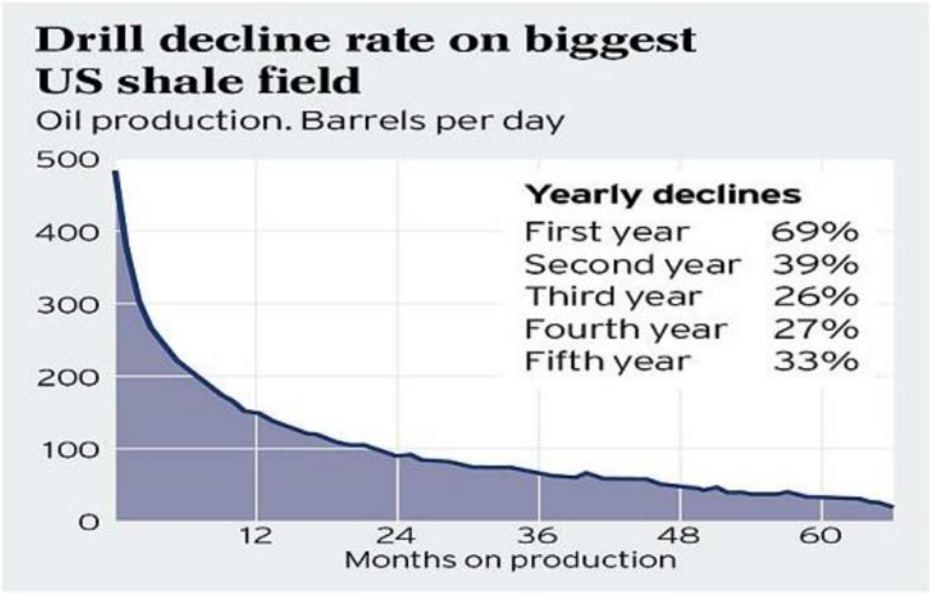

Figure 3—Typical production decline for a shale well

Background and Microproppant Description

The microproppant (MP) used in this study is a small, very strong, perfectly spherical manmade proppant manufactured by Zeeospheres http://www.deepropfrac.com/. A SEM photo of the particles is shown in Figure 4 and the physical properties are described in Table 3. It should be noted that the material has a very high crush resistance (60,000 psi).

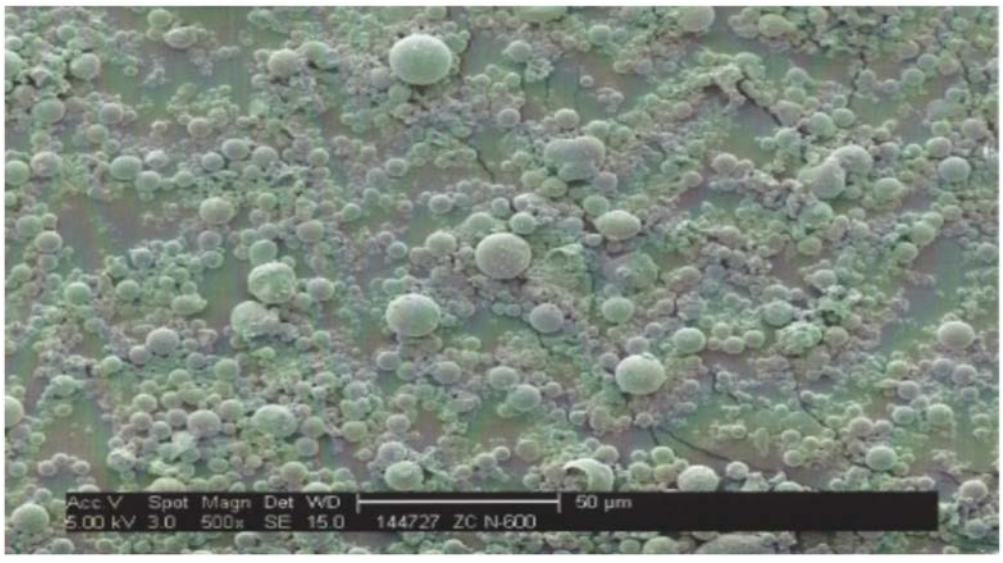

Figure 4—Microproppant SEM photo

Table 3—Microproppant Physical Properties

DEEPROP™ 1000	
D50	25 microns
D95	115 microns
Full Particle Distribution	5-200 microns
Density	2.5 gm/cc
Sphericity	1
Roundness	1
Acid Solubility in 15% HCl	0.80%
Compressive Strength	60,000 psi
Temperature Stability	2200degF

Dahl et.al.[5] recognized and described the utility of this material as a MP in SPE 174060. This paper describes the permeability enhancement of microfractures provided by this MP along with a case history of its use by Devon in the Barnett. Calvin et.al. extended this work in their 2017 paper SPE 184863 which describes its application in the liquids-rich Woodford formation located in the South-Central Oklahoma Oil Province (SCOOP). The production in these wells has continued to be followed and is described in the Case History section of this paper. Stephen Rossenfoss[6] took SPE 184863 and wrote an article about the material in the March 2017 issue of the JPT. This article and these papers caught the attention of the industry and SPE 194340, 189895 and 189832 were all written in 2018. These papers are all university papers and describe a series of tests and placement model evaluations of the material. All are very positive toward the use of the material and clearly show the benefit of using a smaller proppant to increase the propped area of an induced fracture. Work done by Dharmendra. Gonzales, and Ghassemi at the University of Oklahoma (SPE 194340) and shown in Figure 5 and 6 indicates that an additional 16000 square feet in the Eagleford and 8880 square feet in the Utica of fracture area can be propped with the MP when compared to 100 mesh sand [9].

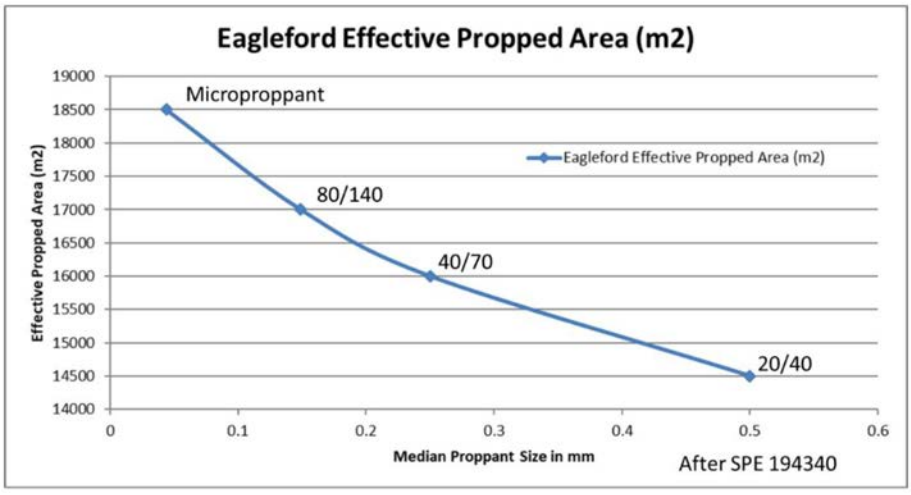

Figure 5—Comparison of the Effective Propped Area vs Proppant Size in the Eagleford

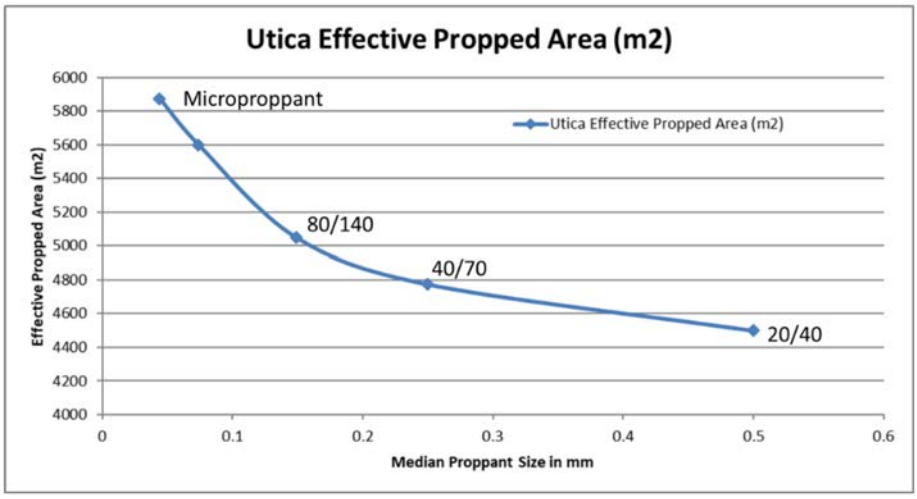

Figure 6—Comparison of the Effective Propped Area vs Proppant Size in the Utica

To determine what this increase in effective propped area might have on productivity, a series of standard and modified conductivity tests were run at an independent testing lab[11, 12]. Figure 7 compares the conductivity of 100 mesh vs MP using a standard ISO test run at 2 lb/ft^2. This would be equivalent to a fracture that has a width of 10,160 microns (0.22 inches). As would be expected, the figure shows the conductivity of the MP to be considerably less than that of 100 mesh, but it should be noted that the 100 mesh loses an order of magnitude of conductivity versus (vs) fracture closure whereas the MP has only a slight loss in conductivity. This loss is probably due to pack rearrangement and not crushing.

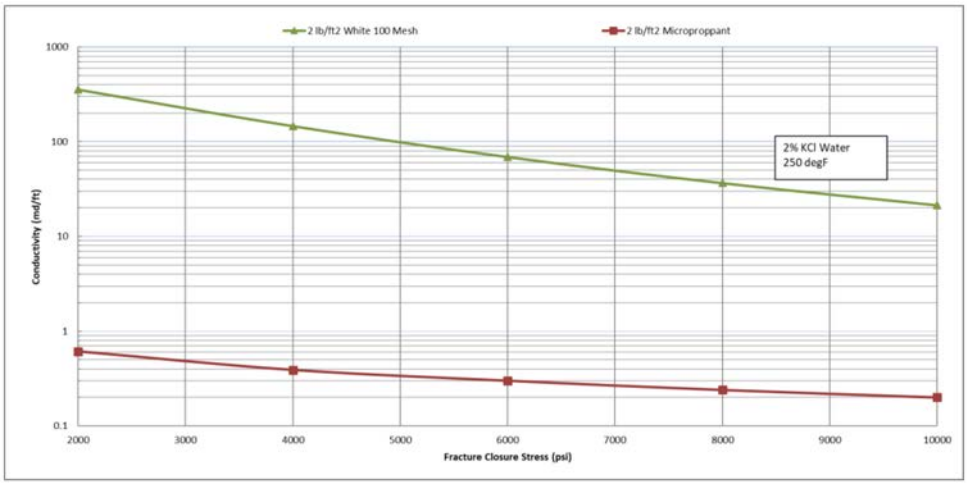

Figure 7—ISO Standard Conductivity comparison of 100 mesh vs microproppant

To determine the conductivity at in-situ conditions, additional tests were run at fracture widths of 1524 microns (0.06 inches) and 355 microns (0.014 inches). All three tests are show in Figure 8. As would be expected the relationship between fracture width and conductivity is linear[15] except at very small fracture widths where the conductivity appears to stabilize. This stabilized conductivity is probably due to the formation of a monolayer.

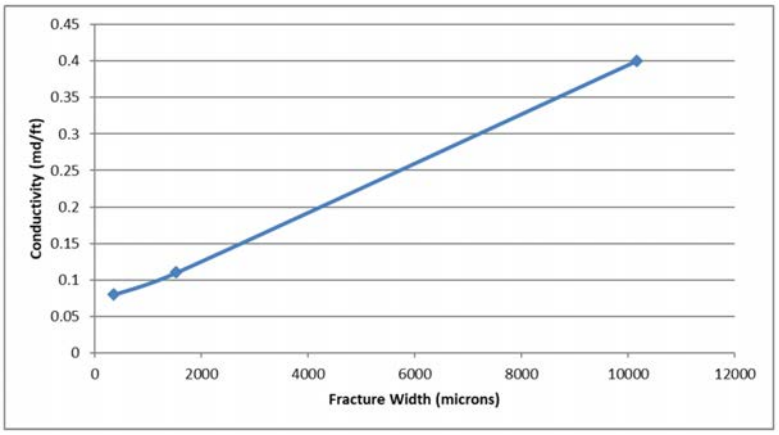

Figure 8—Microproppant Conductivity to kerosene vs Fracture Width at a stress of 3,000 psi and 200°F

To determine the relative conductivity of the MP to water vs oil, an additional conductivity test was run at a width of 1524 microns (0.06 inches). This data is shown in Figure 9. Following the second cycle of kerosene the test was shut-in overnight. The conductivity before shut in is labeled KCl3-a and after shut in KCl3-b. The tests indicate that the conductivity of the MP to oil is twice that of the conductivity to water (0.18 md/ft for oil vs 0.09 md/ft for water). This is quite normal in a system that is water wet.

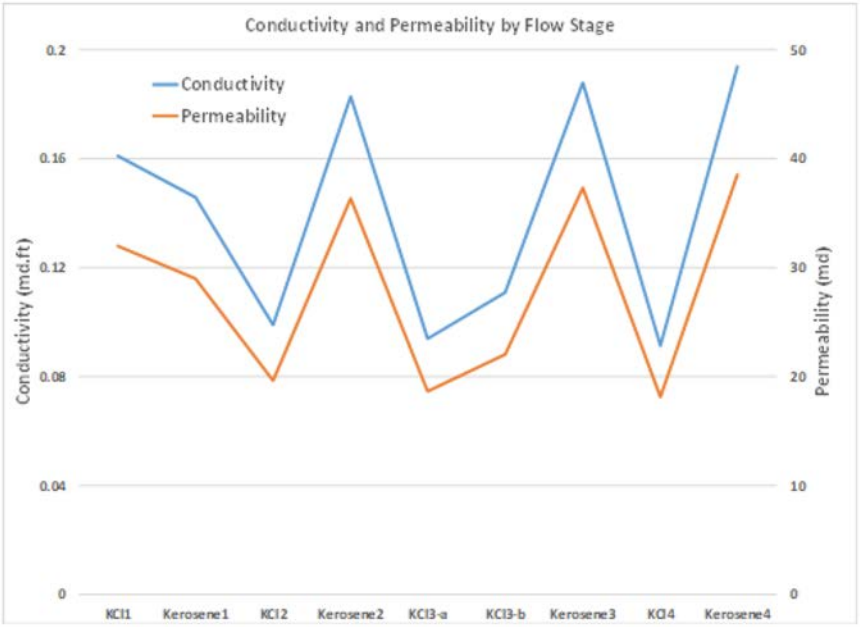

Figure 9—Relative conductivity of microproppant to kerosene vs KCl water at a test width of 1524 microns (0.6 inches)

Using a conductivity of 0.2 md/ft the Fcd (Dimensionless Fracture Conductivity) can be calculated using the equation:

$$F_{cd} = \frac{K_f w}{K x_f}$$

Where:
Fcd = Dimensionless Fracture Conductivity
Kfw = Proppant Conductivity
K = formation permeability
Xf = fracture half length

Figure 10 shows this calculation for a short natural fracture of 100 ft vs the native permeability of the formation. Typically for very low perm unconventional formations a Fcd above 10 is preferred so it is for that reason that the use of MP should be reserved for formations that have native permeabilities less than about 5000 Nano-Darcie's. As shown in Figure 10 it is also recommended that the MP not be used in formations with a modulus less than about 2.5 Million psi because of embedment.

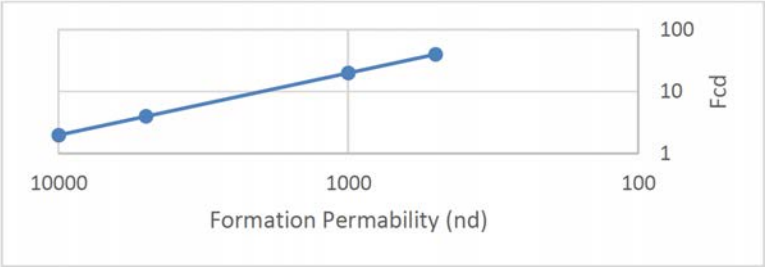

Figure 10—Fcd to Oil vs Formation Permeability at a Xf of 100 ft and a kfw of 0.2 md/ft

Proppant Transport

The settling velocity for various size proppants is shown in Table 4. Because of the size of the material the settling velocity of the microproppant (MP) is much slower than 100 mesh. This allows the material to be transported much deeper into a fracture simply due to better proppant transport.

Table 4—Stoke's Law settling velocity for various proppants

Description	Vs (ft/sec)
20/40 Sand	4.28
40/70 Sand	1.07
80/140	0.22
Microproppant	0.029

μ (cps) = 1
SG of Fluid = 1
SG of Proppant = 2.6

There was some concern about the mixing of the MP into the larger mesh proppant pack as placement occurred so a 48.5″H × 242″L × 0.2″W physical slot flow test was run at FracTech Laboratories http://www.fractech.com located in Woking, United Kingdom. A photo of the test is shown in Figure 11. The behavior of the microproppant was quite unusual because it immediately separated from the 30/50 sand and formed a fluidized bed in front of the sand. As the 30/50 sand dune formed, this fluidized bed was displaced by the front of the 30/50 dune. There was no mixing of the two materials and there was very little, if any, settling of the microproppant.

Figure 11—Physical slot flow model of 30/50 sand mixed with the microproppant

Stimulation Mechanisms

There are four mechanisms that are improving the performance of the wells. These are improved effective propped area, scouring of the near wellbore area resulting in reduced treating pressure, far field diversion and a reduction of convergent flow effects. The first mechanism is well supported by production and modeling data as shown in the case histories and modeling section of this paper.

The scouring and far field diversion are supported by field data. Figure 12 shows a treating plot from one stage in a 44 stage 6 cluster fracture (frac), that was performed in the Delaware basin of West Texas. The red line is the surface treating pressure and the green line is the pump rate. Because the treating string is loaded with the same proppant concentration, and the pump rate is almost constant, it is believed that the surface treating pressure is a fair representation of the downhole pressure behavior. The point that the MP arrives at the perforations and the point where the MP is fully displaced is noted on the plot.

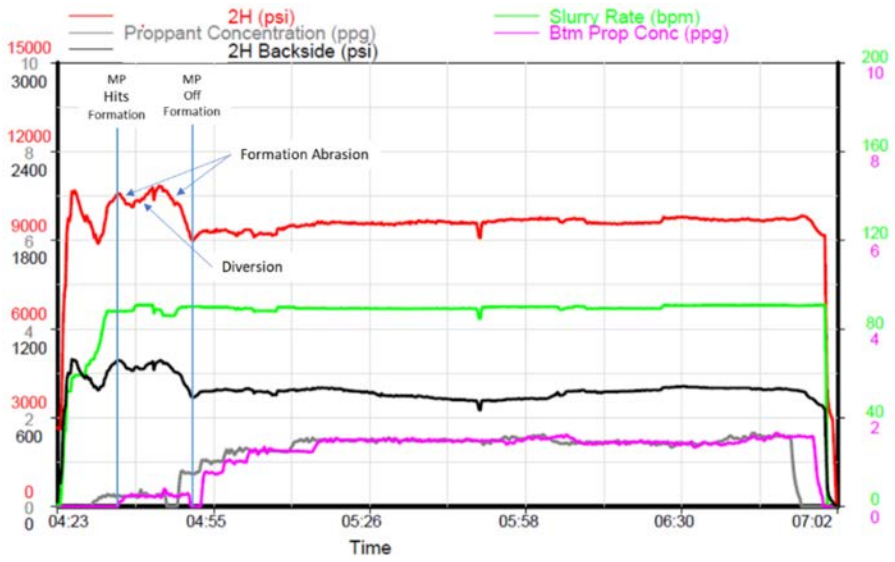

Figure 12—Treating Plot from a treatment in the Delaware Basin showing diversion and formation abrasion when the microproppant hits the formation

Note that when the MP hits the formation, there is a drop in the treating pressure followed by an increase then a sharp drop. It is believed that the initial drop in pressure is due to near wellbore rock abrasion. The increase in pressure is due to bridging and diversion into one or several of the clusters and then the sharp drop is due to additional rock abrasion in the new clusters that were opened by the increase in pressure. Although open to debate because of the very low MP concentration and the Bernoulli effect which concentrates the MP in the center of the flow stream, it is not believed that the pressure drop is due to perforation abrasion. The pressure drop spike noted in the middle of the MP stage looks to be a change in pump rate rather than a reservoir response. Only one of the 44 stages are presented in the paper but most of the stages showed this behavior.

Figure 13 is a treating plot that was presented in SPE 184863[4]. This paper describes the use of MP in the Woodford Shale which is part of the SCOOP play in Oklahoma. The treating pressure drop seen between flags 1 and 2 is due to HCl reacting with the near wellbore rock. The treating pressure drop between flags 2 and 3 is when the MP was being pumped across the formation. As seen with the wells treated in the Delaware basin there also appears to be some cluster diversion occurring as shown by the pressure spikes and break backs. The paper states that this behavior "was consistently observed on the stages where MP was pumped". Discussions with the operator outside the paper indicate that the main reason the operator was using the MP was to reduce pressure screen outs and to allow an increase in the pump rate which improved fluid

efficiency and therefore exposed rock area. It was only after the wells were produced for about 6 months that a production improvement was noted (See Figure 16).

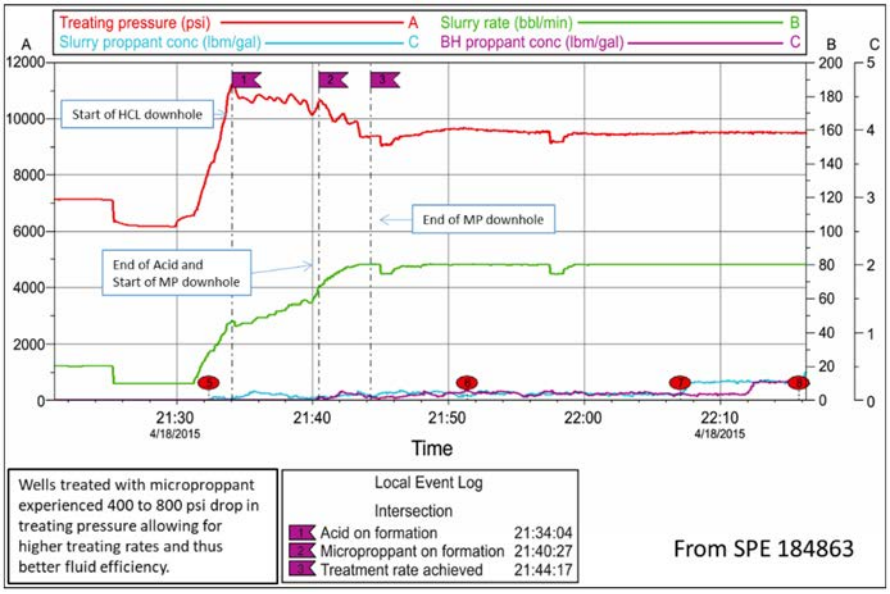

Figure 13—Treating Plot from a treatment in the Woodford (SCOOP) showing formation abrasion when the microproppant hits the formation. Adapted from a plot presented in SPE 184863.

This behavior appears to be formation specific. Wells treated with microproppant in the Marcellus and Utica shales do not exhibit this treating pressure behavior. This may be due to differences in the horizontal stresses where the Marcellus and Utica exhibit less near wellbore tortuosity.

The third proposed mechanism for improving production is a reduction in the near wellbore pressure drop due to convergent flow. The near wellbore erosion of rock caused by the MP may provide channels of improved conductivity around the borehole which would reduce the near wellbore choke caused by the fracture adjusting to the far field stresses as it moves away from the hoop stresses. A build-up and reservoir engineering study to support this theory has not been completed.

On-location Operational Considerations

Manufactured as a dry solid, microproppant (MP) has been pumped in hundreds of wells in the United States across many basins exclusively in a slurry form. Because the MP is so small there was initially some concern about dusting. The MP does not contain any silica so there is no silicosis hazard but there was a concern about product loss. The slurry composition varies by toll blender but generally is an aqueous solution of a viscosifying agent and MP. The MP concentration target is 65% by weight of solution. This translates into roughly 8.2 pounds of microproppant per gallon of slurry.

A MP slurry is viscous and does develop a static gel strength. In the field it flows easily out of an ISO tank through a 3-inch valve and hose when rigged up to a centrifugal pump.

Totes and ISO tankers have been used to transport the MP slurry to well location. A bill of lading provides a net weight of the slurry that, with a certificate of analysis can be converted to gallons. The density of the slurry is 13.5 – 13.6 pounds per gallon.

Mixed to specifications, a MP slurry is readily pumped by a blender's centrifugal pump or could be pulled with other liquid additive pump styles. ISO tank containers are insulated, and experience has shown that MP slurry can be pumped even during harsh winter operations in the short run without heat or longer term when paired with a forced air heater. Initially, the material was added into the pad at a concentration of 0.1

lb/gal which has since increased to 0.25 lb/gal. To minimize water usage, concentrations as high as 0.7 lb/gal are now being used.

There are several different ways to introduce MP into a well. The most common way has been to pump the MP slurry from an ISO tank container or tote tank with a centrifugal pump that provides boost pressure via a suction manifold to a high pressure, high rate pump truck. Some frac pump trucks are equipped with a centrifugal pump mounted on a rear fender eliminating the need for a separate centrifugal pump, like one that would be backup for the blender. The slurry gets pumped into a missile manifold where it is proportioned in the frac fluid by varying the gallons pounds of microproppant added by slurry to the total fluid rate.

A second option would be to pull the slurry from the ISO tank container with the blender's suction pump and add the MP at design concentration on-the-fly with the rest of the incoming water from the frac tanks. Depending on the frac service provider, the MP slurry would be pumped by all pumps or a bank of pumps designated for pumping proppant during any given stage or frac.

A third option is to add the MP as a dry material to the sand hopper via a silo or box system. This has yet to be tested but would reduce transportation and product cost. Initially, operators resisted any attempt to run such a fine particle under dust collection for fear of losing too much material. However, with current market forces and the push for lower costs it likely won't be long before a more conventional process of adding the MP is tried.

Bypassing the blender tub may not be a desirable means to add MP as there will be no blender proppant concentration to display in the treatment van. An additional concern is that an inline densometer may not be calibrated or it simply may fail to properly display low microproppant concentrations often applied to resource play wells.

Case Histories

To date the microproppant (MP) discussed in this paper has been pumped in the Barnett, Woodford (SCOOP), Utica, Marcellus and Wolfcamp (both the Delaware and Permian basins) shales. The Wolfcamp wells have not produced long enough to provide any definitive data but in all the other cases there is at least 12 month or longer data available. Some early Wolfcamp Delaware basin data is shown in Figure 23,

Case 1 – Barnett Shale

This is a 11 well trial that Devon conducted in Wise County, Texas. It was the first set of wells that was reported in the literature and is fully described by Dahl et.al in SPE-174060-MS[5]. Four of the wells were treated with microproppant (MP) with the remaining seven offset wells used as a control. In these treatments, 4,200 lb of MP mixed in a liquid slurry was added to the pad at a concentration of 0.1 lb/gal. The ID and API numbers of the study wells was determined utilizing FracFocus https://fracfocus.org/. Once the wells were identified, available production data was gathered using NavPort® which is now associated with the RS Energy Group https://www.rseg.com/. This data was converted to BOE, normalized so that the production started at the same time and plotted. Rather than show all the wells, Figure 14 shows the average cumulative BOE production for the four MP wells vs the seven offset wells. As can be seen in the plot, the wells start at about the same point but start to separate with the uplift continuing to improve over time. This is consistent with the idea of having a larger conductivity propped fracture area.

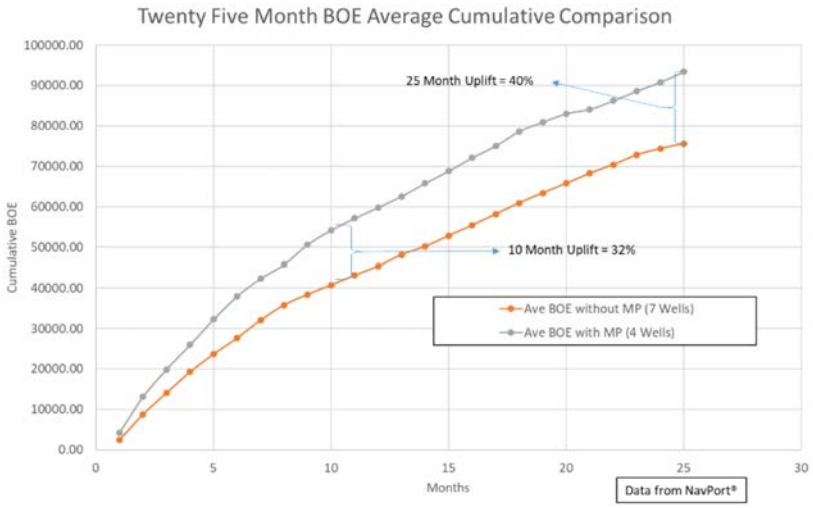

Figure 14—Twenty Five Month BOE Average Cumulative Production of the 11 wells used in the Barnett Shale study.

The lateral length of these wells varied from 3792 ft to 5252 ft for the MP wells and from 3952 to 6124 for the offset wells. Figure 15 is an attempt to normalize the data on a per foot basis and then compare the data for all wells using a lateral length of 4000 feet.

Normalized/foot Barnett Shale 25 Month Cum Production*

Well Number	1H	2H	3H	4H MP	5H	6H MP	7HA	8HA MP	9HB MP	10HB	11HB	Total	Average
Lateral Length in feet	4302	3922	3952	3902	4502	3792	5712	5252	4102	4902	6124		
25 Month Cum Production (BOE)	62334	68411	71649	59797	63852	82091	63062	96930	134786	61198	138743		
Cum Production (BOE) per foot of Lateral	14	17	18	15	14	22	11	18	33	12	23		
Cum Production (BOE) per 4000 foot of Lateral	57,958	69,772	72,519	61,299	56,732	86,594	44,161	73,823	131,434	49,937	90,623		
Wells without Micoproppant	57,958	69,772	72,519		56,732		44,161			49,937	90,623	441,702	63,100
Wells with Micoproppant				61,299		86,594		73,823	131,434			353,150	88,288
% Increase with Micropoppant													40%
Average production increase in BBLs													25,187

* Production data from Navport®

Figure 15—Twenty-Five Month BOE Average Cumulative Production of the 11 wells used in the Barnett Shale study normalized to a per foot basis.

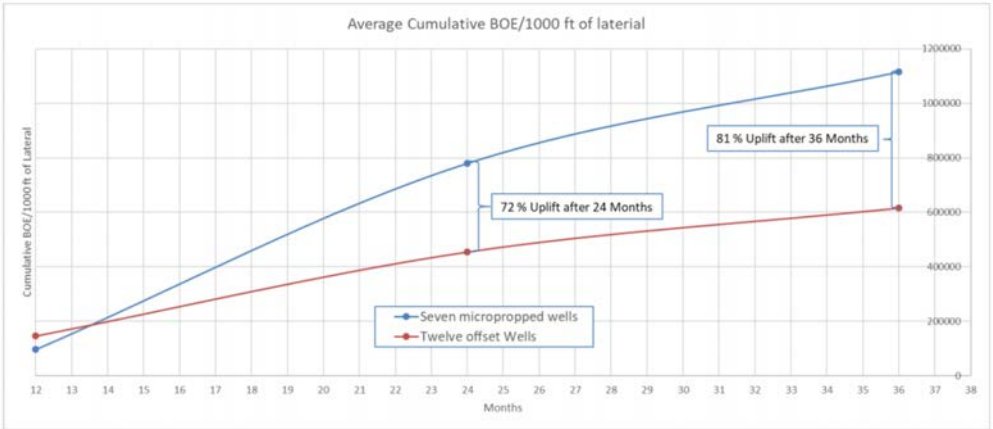

Figure 16—Woodford (SCOOP) averaged cumulative BOE/1000 foot of lateral for 7 MP wells and 12 offset wells

Case 2 – Woodford Shale (SCOOP)

Three operators have used the microproppant in the Woodford SCOOP located in Oklahoma. One operator wishes to keep the data confidential so that data is not presented here.

Study 1 - The first operator conducted a study using 7 MP wells offset by 12 wells. This work was first reported on by Calvin et.al. in SPE 184863. As with the Barnett wells 4200 lbs of the MP was added as a liquid slurry into the pad at a concentration equivalent to 0.1 lb/gal. Once the API numbers for all wells were determined, the production data was gathered from the Oklahoma Tax Commission website https://otcportal.tax.ok.gov/gpx/index.php. Twelve-month data is available on the website, but older data can be purchased by contacting the tax commission. The data was converted to BOE, was plotted for all wells and normalized to BOE/1000 ft of lateral. That data is shown in Figure 16.

Unlike the Barnett wells, it took about 12 months before the wells treated with the MP began to outperform the offset wells but after that the results are remarkable. The main reason this operator was using the MP was to reduce the treating pressure as shown in Figure 13. The pressure limit on the wellbore was 11,500 psi but the MP removed about 800 to 1100 psi treating pressure which allow the treatment to be placed at a higher pump rate which improved fluid efficiency which exposed more rock. It was not until 6 months after the treatments that the production improvement was noted.

In addition, type curves were developed utilizing the PHDWin® software offered at http://www.phdwin.com/ for all wells. This data set is too large to present in this paper but an example 10-year gas type curve projection for one of the well pairs is presented in Figure 17.

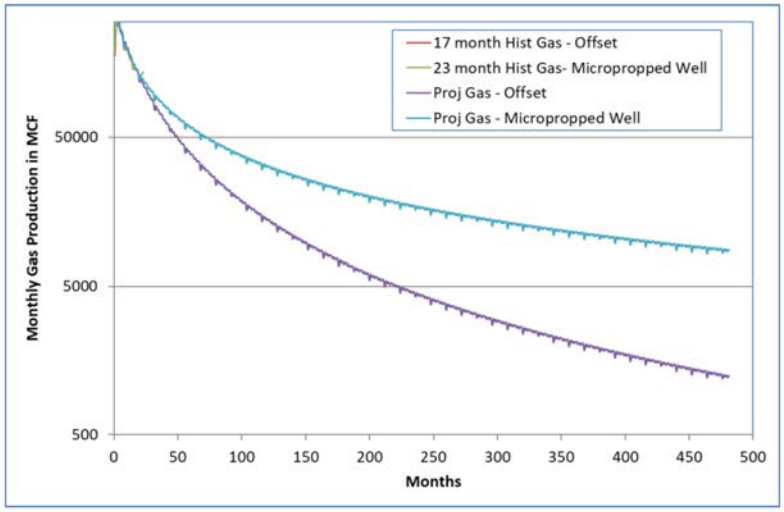

Figure 17—Woodford (SCOOP) type curve gas projection for one well pair in the 19 well study.

Study 2 – This study consisted of 3 microproppant (MP) wells and 6 offset wells completed in the oil leg of the Woodford (SCOOP) West of Study 1. The study and offset wells were carefully selected to try and keep the geology and well geometries and orientations as consistent as possible. The wells were completed with 20 stages pumped at 80 BPM. Each stage utilized 120,000 pounds of 100 mesh followed by 371,000 pounds of 40/70 mesh sand with a mixture of Guar and FR as the carrying fluid. On the wells that received microproppant, 8200 pounds was pumped in the pad of each stage at an average concentration of 0.45 ppg. The cumulative oil production for all wells normalized to the same start date is shown in Figure 18.

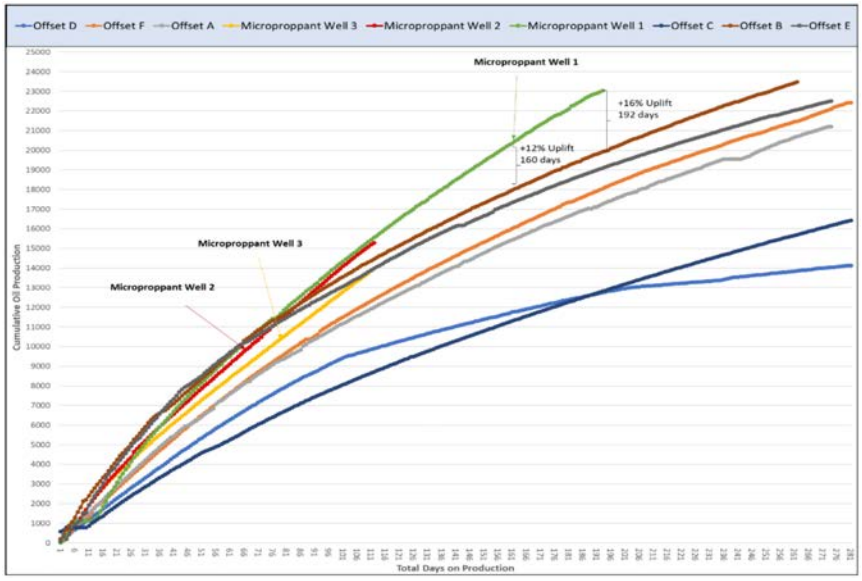

Figure 18—Woodford (SCOOP) nine month averaged cumulative oil production for 3 MP wells and 6 offset wells

This data was provided to the authors by the E&P company. As can be seen in the figure, the wells that received the MP initially behaved like the offset wells and then began to separate as the lower decline rates became evident.

Case 3 – Utica Shale (Ohio)

This study consisted of 2 micropropped (MP) wells and 1 offset. The wells are in Eastern Ohio where the Utica is located at about 7500 ft TVD. The offset well had a lateral length of 7845 ft and was fractured using 45 stages spaced 180 foot apart. Each stage had 5 clusters spaced 36′ apart. The first MP well had a lateral length of 5742 feet and was designed to have 44 stages spaced 150 ft apart. Each stage had 5 clusters spaced 30' apart. This well had several pressure issues so that only 39 of the planned 44 stages were fraced. The second MP well had a lateral length of 7341 ft and was fraced using 48 stages spaced 150 foot apart. Each stage had 5 clusters spaced 30 ft apart. Stage 7 was skipped so that only 47 of the planned 48 stages was fractured. Figure 19 and 20 show the cum oil and gas for the three wells. The offset well had some downtime, so the data is formatted to eliminate this downtime effect.

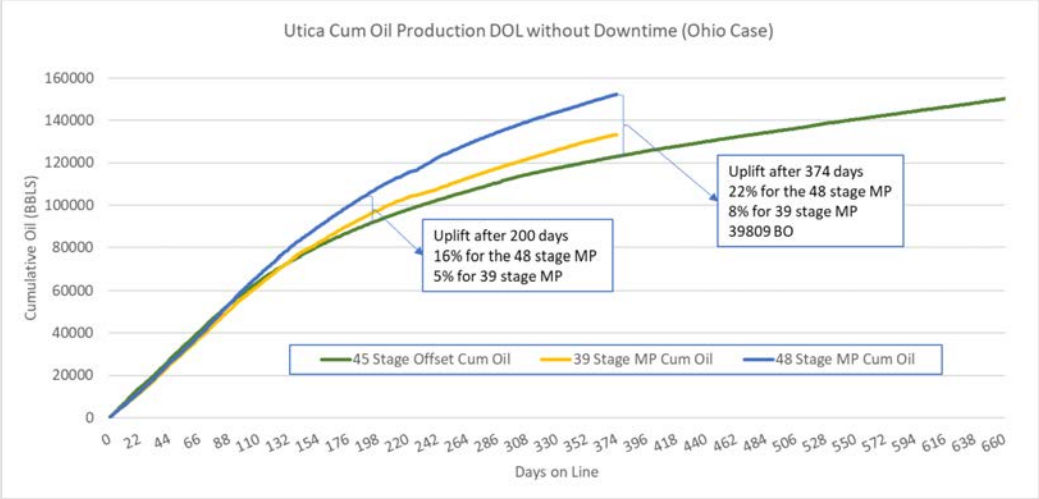

Figure 19—Cumulative Oil for the Eastern Ohio case.

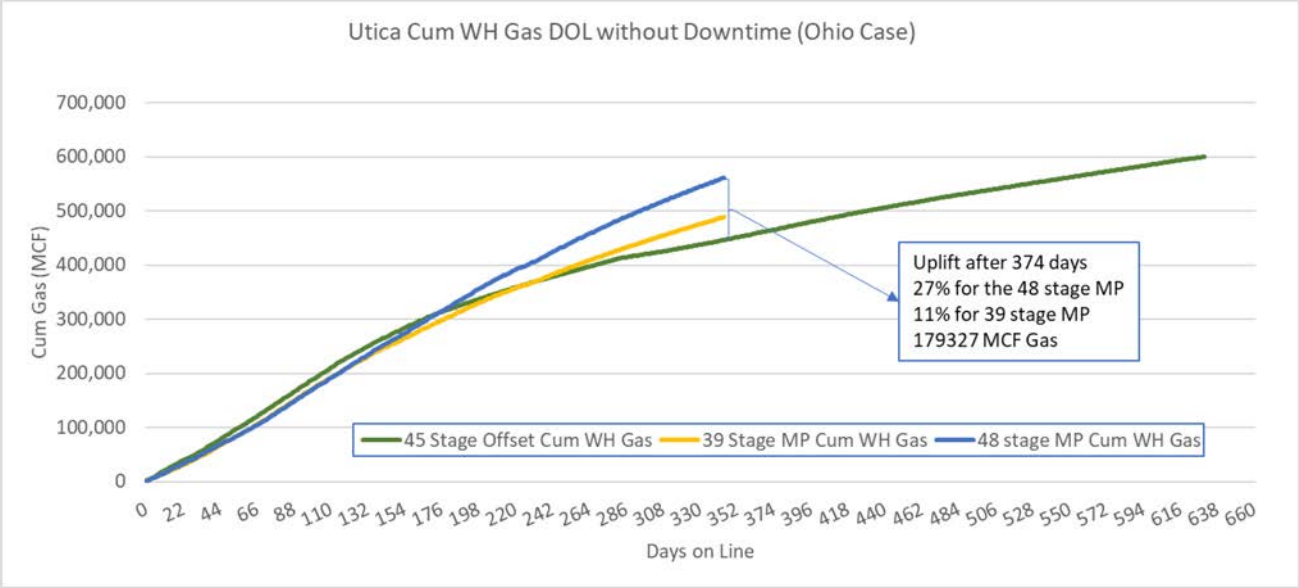

Figure 20—Cumulative Gas for the Eastern Ohio case.

Case 4 – Marcellus (Pennsylvania and West Virginia)

This study consisted of a test of 16 wells on two pads in Pennsylvania and 14 wells on four pads in West Virginia. In the Pennsylvania case 6 of the 16 wells were treated with 7500# of microproppant (MP) used in each stage. In the West Virginia study 7 of the 14 wells were treated with 7500# of MP used in each stage. There were 50 to 60 stages completed in each of these wells. Figure 21 and 22 shows an example of 14 month (Pennsylvania) and 8 months (West Virginia) cum production for two pads in the study. On all pads and in all cases the data indicates that the MP treated wells are performing about on par with the offset wells. Subsequent to these results some modeling work, which is described in the modeling section below, showed that the microfracture structure in the Marcellus is very limited and that it is difficult to create any degree of complexity in the Marcellus.

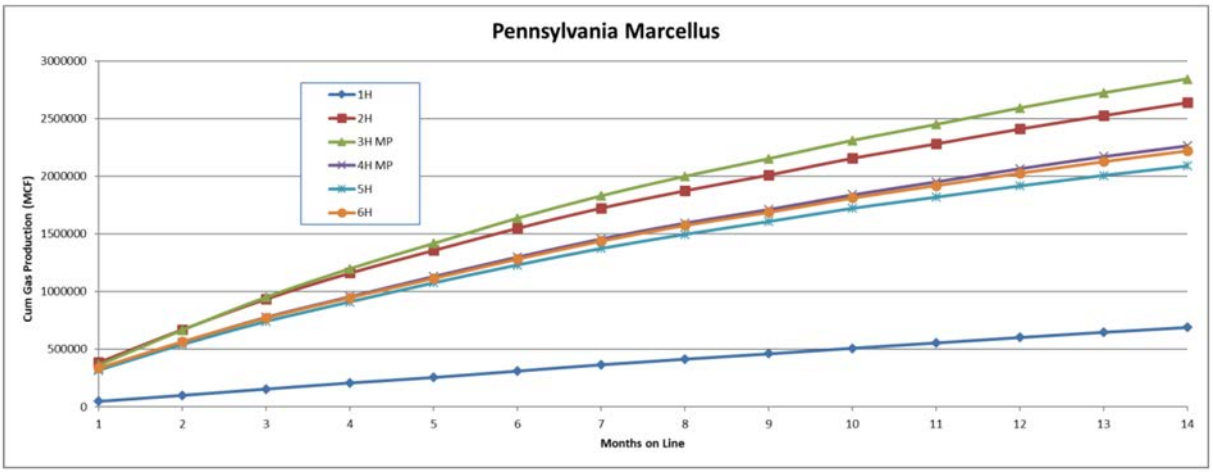

Figure 21—Cumulative Gas for one pad in the Pennsylvania Marcellus

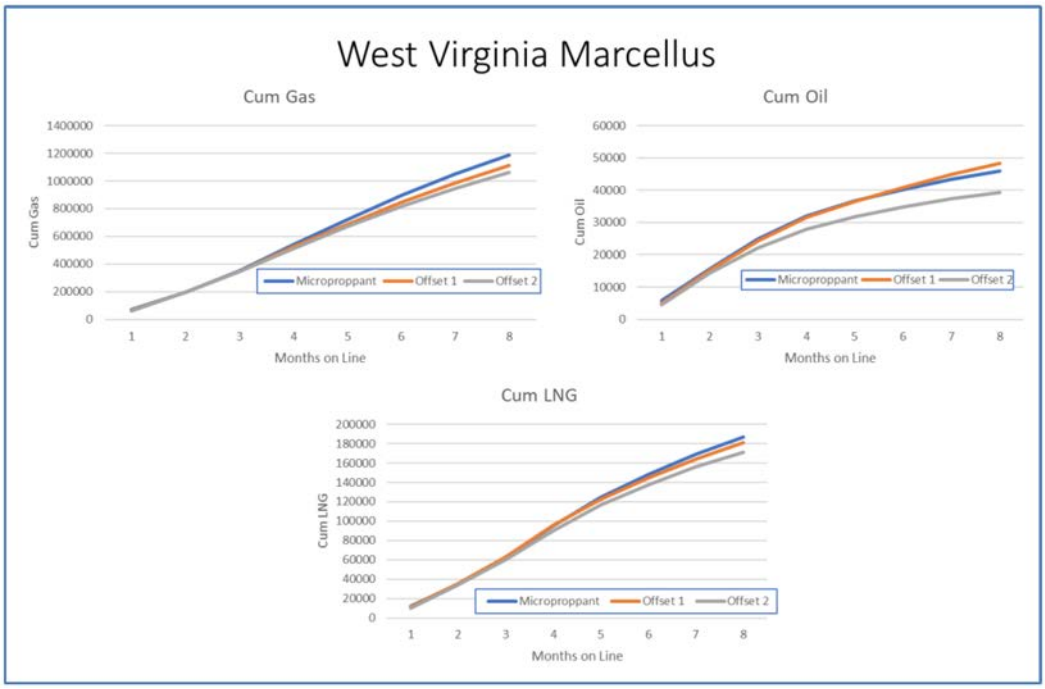

Figure 22—Cum gas, cum oil and cum LNG for a three-well test in West Virginia.

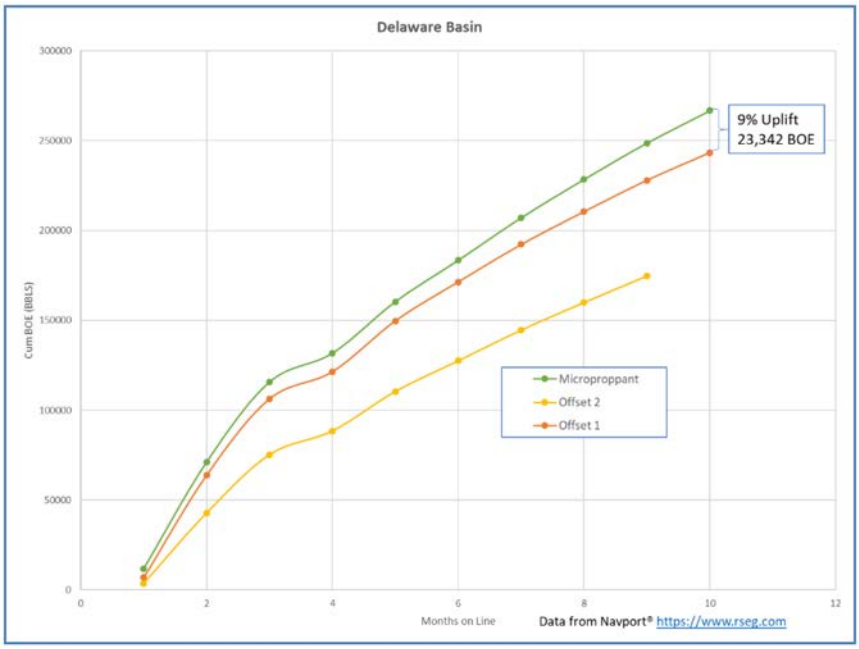

Figure 23—Cum BOE for a three-well test in the Wolfcamp Delaware Basin.

Case 5 – Permian/Delaware Basin

There are currently five tests being conducted in the Permian Wolfcamp, two in the Permian basin and three in the Delaware basin. Four of these tests have not been on production long enough to provide definitive data but the preliminary results are encouraging. One test being conducted in the Delaware Basin currently has ten months of production data and the results are shown in Figure 23. The data was gathered via Navport® https://www.rseg.com.

Simulated Results

No attempt was made to history match the results described above because the detailed log and reservoir data was not available for such a study. Rather typical wells were used[1] and stresses, rock properties, reservoir properties, were maintained consistent with the two formations studied.

Marcellus.

The first formation studied was a typical Marcellus well, with the well presumed to be drilled in a strike-slip geologic environment. Given this, the maximum horizontal stress was set to be slightly higher than the overburden, and the results are "nothing". Pressure in the main hydraulic fracture never reached a level sufficient to create any dilated natural fracture width resulting in the micro-proppant having no effect.

Barnett.

A typical Barnett well was defined, using the logs and properties from Reference 1. This case was simplified to just consider a 200′ thick Lower Barnett interval. The undilated natural fracture properties were also taken from Reference 1. A cross section showing placement of the micro-proppant is seen in Figure 24.

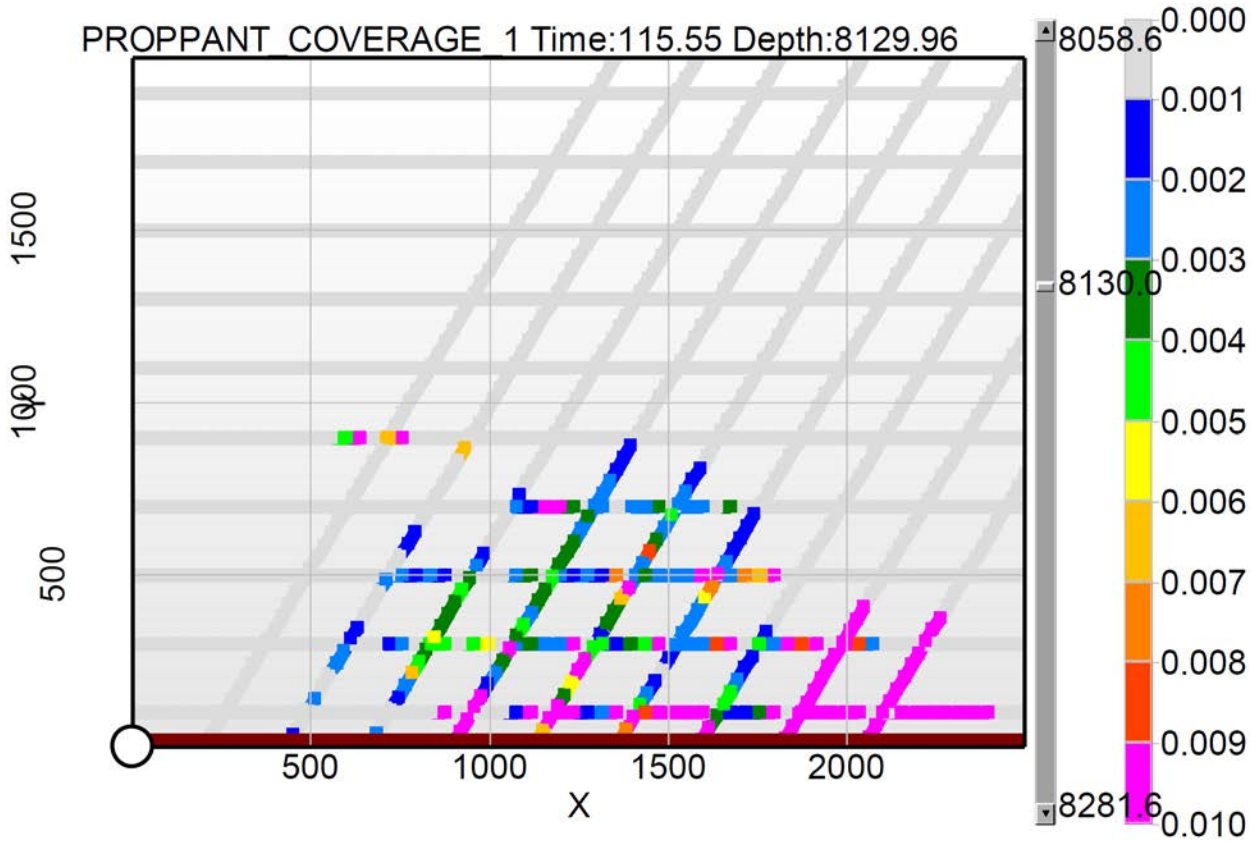

Figure 24—Placement of micro-proppant (lb/ft²) at mid-depth of 200′ thick Lower Barnett.

Clearly, consistent with the 4200# volumes pumped, the proppant coverage is well down into a partial mono-layer regime. Thus, a straight coverage → conductivity relation is not appropriate. The effects of such small proppant amounts have been recently studied experimentally.[20] This showed that just isolated particles, and clumps of micro-particles, could increase the permeability of the unpropped fracture by a factor of 10x. This was used for the resulting reservoir simulations seen in Figure 25 and 26. Note that lessor concentrations near the wellbore resulted from the natural fracture opening not occurring early enough.

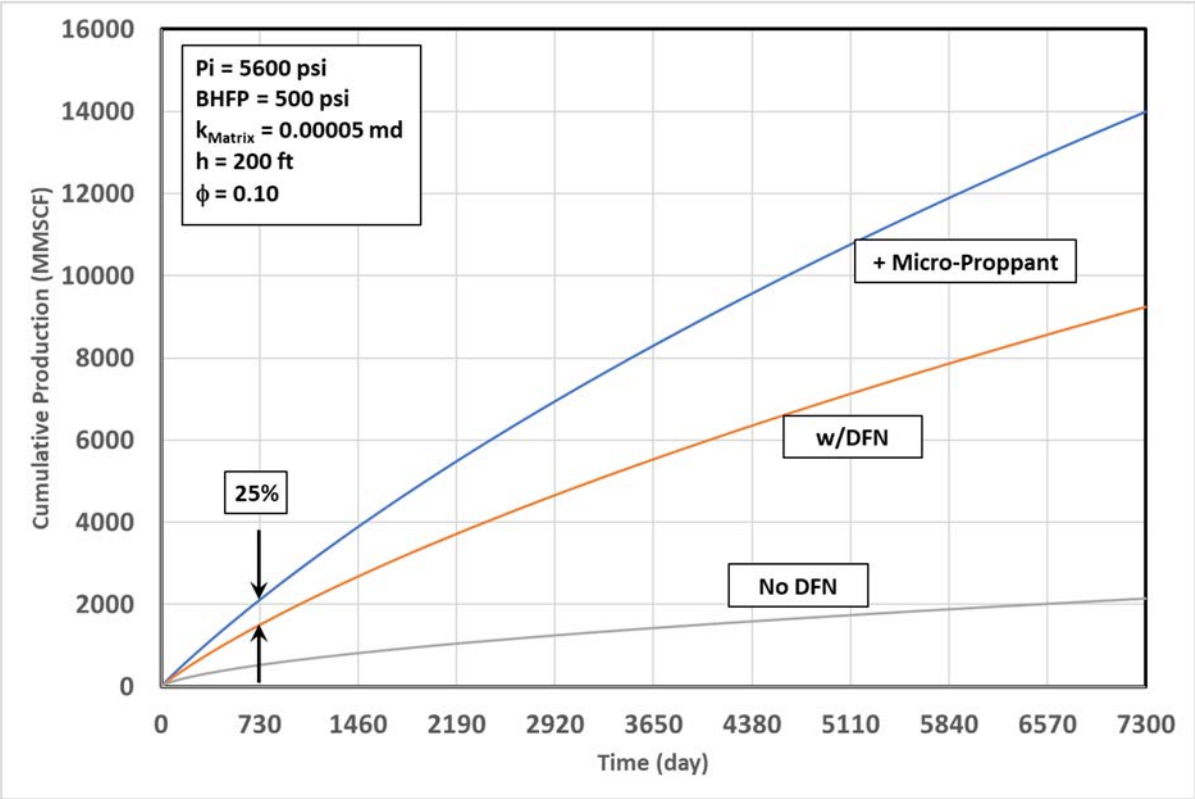

Figure 25—Effects of micro-proppant on post-frac production

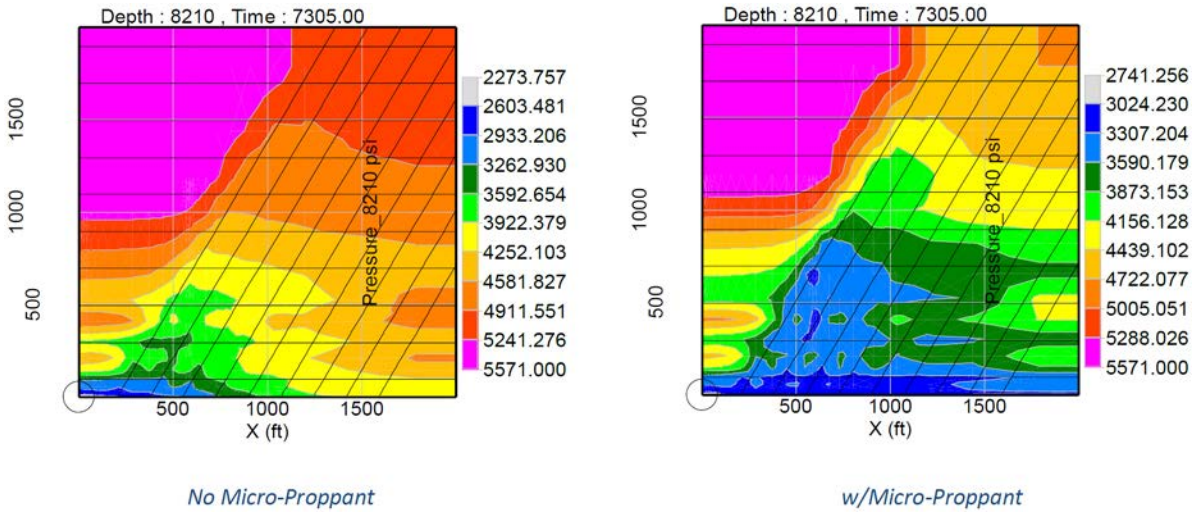

Figure 26—Effects of micro-proppant on reservoir drainage

Conclusions

1. A new discrete fracture network model which includes dynamic proppant transport has been developed.
2. The dynamic proppant transport model has found utility in identifying which shale reservoirs will benefit from the use of a microproppant.
3. The microproppant used in this study resulted in significant uplift and reduced production declines in the Barnett, Woodford (SCOOP), Utica and Permian Basin shales.

4. In addition to uplift, pressure pumping data indicates that the microproppant used in this study proved near wellbore scouring and diversion in some reservoirs.

Acknowledgements

The authors would like to thank NSI Technologies for the use of their discrete fracture network module which is included in the software package StimPlan™ http://www.nsitech.com/ and Zeeospheres http://www.deepropfrac.com/ who manufactures the microproppant used in this study under the trademark Deeprop® 1000 for sponsoring much of the work presented in this paper.

References

1. Britt, Larry K., Smith, Michael B., Klein, Henry H., Deng J.Y. 2016 Production Benefits from Complexity - Efficts of Rock Fabric, Managed Drawdown and Propped Fracture Conductivity, presented at the SPE Hydraulic Fracturing Technology Conference and Exhibition held in The Woodlands, Texas USA, 9-11 February 2016. SPE-179159-MS.
2. Evans-Pritchare, Ambrose, *Commodity Supercycle in Rude Health Despite Shale, The Telegraph*, 31 July 2013. https://www.telegraph.co.uk/finance/comment/ambroseevans_pritchard/10214989/Commodity-supercycle-in-rude-health-despite-shale.html
3. Sone H. and Zoback M., Mechanical properties of shale-gas reservoir rocks - Part 2: Ductile Creep, Brittle Strength and their Relation to the Elastic Modulus, *Geophysics* **78**(5):393–D402, September 2013
4. Calvin, J., Grieser, B., and Bachman, T. 2017. Enhancement of Well Production in the SCOOP Woodford Shale through the Application of Microproppant. Presented at the SPE Hydraulic Fracturing Technology Conference and Exhibition, The Woodlands, Texas, USA, 24-26 January. SPE-184863-MS. https://doi.org/10.2118/184863-MS.
5. Dahl, J., Nguyen, P., Dusterhoft, R., Calvin, J. et al. 2015. Application of Micro-Proppant to Enhance Well Production in Unconventional Reservoirs: Laboratory and Field Results. Presented at SPE Western Regional Meeting, Garden Grove, California, USA, 27-30 April. SPE-174060-MS. https://doi.org/10.2118/174060-MS.
6. Rassenfoss, Stephen, *Testing Tiny Grains Seeking More Output, Journal of Petroleum Technology*, Society of Petroleum Engineers, March 2017, pp 28–33.
7. Calvin, J., Grieser, W., and Bachman, T., 2017. Enhancement of Well Production in the SCOOP Woodford Shale through the Application of Microproppant. Presented at SPE Hydraulic Fracturing Technology Conference and Exhibition held in The Woodlands, Texas USA, 24-26 January 2017. SPE-184863-MS.
8. Brice Y. Kim and I. Yucel Akkutlu, Texas A&M University; Vladimir Martysevich and Ron Dusterhoft, Halliburton, Laboratory Measurement of Microproppant Placement Quality using Split Core Plug Permeability under Stress, presented at the SPE Hydraulic Fracturing Technology Conference and Exhibition held in The Woodlands, Texas USA, 23-25 January 2018. SPE-189832-MS.
9. Dharmendra K., Gonzales, Ruben A. and Ghassemi, Ahmed, The University of Oklahoma; The Role of Micro-proppants in Conductive Fracture Network Development, presented at the SPE Hydraulic Fracturing Technology Conference and Exhibition held in The Woodlands, Texas USA, 5-7 February 2019. SPE-194340-MS.
10. Shrivastava, Kaustubh and Sharma, Mukul M.; Proppant Transport in Complex Fracture Networks, presented at the SPE Hydraulic Fracturing Technology Conference and Exhibition held in The Woodlands, Texas USA, 23-25 January 2018. SPE-189895-MS.

11. Fisher, C. Short-Term Conductivity Testing for Zeeospheres Ceramic Microspheres, *Constien and Associates Laboratory Report* "https://www.candalab.com/", March 11, 2016.
12. Fisher, C. Relative conductivity Testing for Zeeospheres Ceramic Microspheres, *Constien and Associates Laboratory Report* "https://www.candalab.com/", December 2, 2018.
13. Van der Vlis, A. C., et al, "Criteria for Proppant Placement and Fracture Conductivity," 50th Annual Meeting of SPE, Dallas, Texas, Sept. 28-Oct. 1, 1975.
14. Gruesbeck, C. and Collins, R. E., "Particle Transport Through Perforations," SPE 7006, presented at 3rd Symp. on Formation Damage Control, Lafayette, Feb 15-16, 1978.
15. 2005 *StimLab proppant consortium report* https://www.corelab.com/stimlab/proppant-consortium
16. *Technical Service Report P475, Evaluation of Zeeospheres Zeta Potential, Premier Oilfield Fluids Laboratory*, May 2, 2018
17. Smith, M.B., and Klein, H.H.: "Practical Application of Coupling Fully Numerical 2-D Transport Flow Calculations with a Pseudo-3-DFracture Geometry Simulator," paper SPE 30505 presented at the1995 SPE Annual Technical Conference and Exhibition, Dallas, 22-25 October.
18. M. B. Smith, NSI Technologies; A. Bale,, Statoil; L. K. Britt, Amoco Production Co., B. W. Hainey, Arco E&P Technology; H. K. Klein, Jaycor, "Enhanced 2D Proppant-Transport Simulation:The Key To Understanding Proppant Flowback and Post-Frac Productivity," paper SPE 38610 presented at the 1997 SPE Annual Technical Conference and Exhibition, San Antonio, Texas, 5-8 October
19. M. B. Smith, NSI Technologies; A. B. Bale, STATOIL; L. K. Britt, SPE, Amoco Production Co; H. H. Klein Jaycor.; E. Siebrits, SPE, Schlumberger; and X. Dang, Jaycor: "Layered Modulus Effects on Fracture Propagation, Proppant Placement, and Fracture Modeling,", paper SPE 71654 presented at the 2001 SPE Annual Technical Conference and Exhibition, New Orleans, Louisiana, 30 September-3 October 2001
20. Dahl, Jeff, Devon Energy; Philip Nguyen, Ron Dusterhoft, James Calvin, Shameem Siddiqui, Halliburton; "Application of Micro-Proppant to Enhance Well Production in Unconventional Reservoirs: Laboratory and Field Results", SPE 174060, presented at SPE Western Regional Meeting held in Garden Grove, California, USA, 27-30 April 2015.

Appendix A

Simulation

The hydraulic fracture simulation model incorporates a Discrete Natural Fracture Network intersecting the hydraulic fracture (HF) at various locations along its length. The details of the stand-alone HF model are presented in Ref. [1, and 17–19]. The combined HF/DFN modeling capability allows for the impact of the stimulation on the natural fracture network and the assessment of the subsequent production.

Consider the illustration in Figure A-1. This shows an ideal hydraulic fracture propagating away from a wellbore. As it propagates, the hydraulic fracture crosses multiple natural fractures (shown in this ideal picture as consisting of two sets, each set with a common dip/strike, one set parallel to the main hydraulic fracture). At each intersection, fluid begins to leak-off into the natural fracture. This reduces effective stress acting to close the natural fracture, thus allowing permeability of the natural fracture to increase – increasing fluid loss from the main fracture, etc. While simplistic in comparison to actual natural fracture distributions, the simulation allows some assessment as to the magnitude of additional fluid loss, determination of any DFN opening, and an assessment of the effects on post-frac production. As fluid pressure along the natural fractures continues to expand their area/volume and increase their magnitude, two important points are eventually reached.

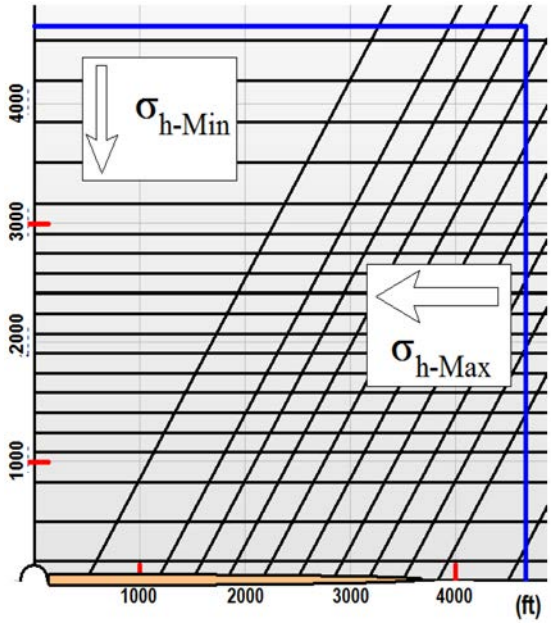

Figure A-1—Fracture Network Simulation Capability

Critical State – At some point increased fluid pressure may reduce the effective stress along the natural fractures to a point where active slippage may occur. This might be visible as micro-seismic emissions and would probably provide a permanent path of increased permeability leading back to the hydraulic fracture.

Fracture Opening – With an even higher pressure, the pressure may exceed the stress acting normal to the natural fracture, and this natural fracture may begin to dilate or open. At this point, it might be possible to place some proppant (albeit small proppant such as micro-proppant or 100 mesh sand) into the natural fractures and preserve this increased fracture flow capacity.

The reduction in critical stress, the impact of exceeding critical stress, the dilation of natural fractures at higher pressures, and proppant placement in the natural fractures are all considered when calculating the impact on production of the stimulated fracture network.

The natural fracture model consists of a network of clusters of intersecting planes. Each cluster has a specific height, strike, dip, number per length, span, starting and ending points. The cluster can intersect the hydraulic fracture at arbitrary locations along its length or intersect other clusters.

The strike and dip of the natural fracture sets, as well as their density and spacing, are specified based on the available well and geological information. These can be varied orthogonally and parallel to the hydraulic fracture to describe more complex fracture networks.

The simulation tracks fluid loss from the "main" hydraulic fracture into the connected system of natural fractures. As the pressure builds in the natural fracture the local width can increase from the initial undilated width.

The natural fractures are simulated as parallel planes of varying width separating the planes. This fluid flow is tracked in two dimensions throughout the planes. The increase in pore pressure along the natural fractures is also simulated as part of this flow, allowing permeability of the undilated fracture to increase as effective stress is reduced. Eventually, fluid pressure at some points may increase sufficiently to overcome normal stresses acting on the natural fractures, and actual dilated (open) fracture widths may develop. When this occurs, the model calculates a "pseudo width" or "virtual width" for the affected natural fracture assuming the local width of the natural fracture is a simple function of the pressure, local stress, natural fracture height, and rock modulus.

The solution algorithm fully couples the HF/DFN flow/pressure solution.

The "undilated" permeability for the natural fractures is specified as a curve of permeability (or flow capacity or "undilated width") versus effective stress. Ideally this data must come from lab tests on core samples with actual natural fractures. Opportunities for this are obviously rare. Thus, artificially created fractures in core samples may be used to at least give some idea of undilated permeability behavior (probably a lower bound).

Flow in the Natural Fractures.

For the local natural fracture permeability, we assume flow between parallel plates for the leak-off fluid. The profile for laminar flow between parallel plates is parabolic, Figure A-2.

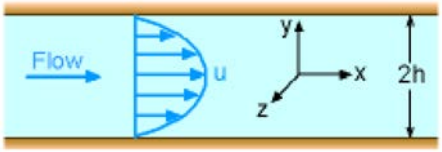

Figure A-2—Parabolic velocity profile between parallel plates

With the pressure drop Δp, the x-velocity at any vertical point is

$$u = \frac{1}{2\mu}\frac{\partial p}{\partial x}\left(y^2 - h^2\right)$$

The flow rate per unit length along the plate is the vertical integral of the velocity

$$q = \int_{-h}^{h} u = -\frac{2h^3}{3\mu}\left(\frac{\partial p}{\partial x}\right)$$

If the width w = 2h, then the average velocity at any length along the plates is

$$\overline{u} = \frac{\int_{-h}^{h} u\,dy}{w} = -\frac{w^2}{12\mu}\left(\frac{\partial p}{\partial x}\right)$$

Or in Darcy form

$$\overline{u} = -\frac{k}{\mu}\left(\frac{\partial p}{\partial x}\right)$$

Similarly, in the velocity in the "z" direction is

$$\overline{v} = -\frac{k}{\mu}\left(\frac{\partial p}{\partial z}\right)$$

The local natural fracture permeability is that between parallel plates, i.e.,

$$k_{nf} = \frac{w_{nf}^2}{12}$$

The viscosity of the fluid is that of fracturing fluid. Using these expressions for permeability and width inside natural fractures along with the density/intensity of the natural fractures along hydraulic fracture length, the fluid flow equations can be coupled to those in the hydraulic fracture, giving a self-consistent solution for the pressure throughout the hydraulic/natural fracture system. Thus, as the pressure inside the hydraulic fracture increases, leak-off into the natural fracture will increase the pressure and width inside the natural fracture, in turn affecting the pressure and leak-off inside the main hydraulic fracture, etc.

Finally, the fluid lost from the natural fractures to the matrix is also calculated (based on assuming "Carter", C/√Time loss). Since natural fractures are generally only of concern in hard, "tight" formations, this simple fluid loss approach (for fluid flowing from the natural fractures into the formation matrix) seems fully justified.

Pseudo 3D Pressure-Width.

As fluid leaks off into the natural fracture, fluid pressure in the natural fracture increases, decreasing the effective stress acting to close the natural fracture and allowing the natural fracture permeability to increase. At some point, fluid pressure inside the natural fracture may exceed the normal stress acting to close that natural fracture. Since the pressure in the natural fracture is not uniform vertically and the rock properties might not be uniform vertically, we have incorporated a Pseudo 3D model of width vs. pressure over the natural fracture height. The closure stress is the stress normal to the natural fracture face determined from the orientation between minimum and maximum horizontal stresses. The equation coupling pressure to width is

$$\left[K_{ij}\right]\ \left[w_j\right] = \left[p - \sigma_N\right]_i$$

where K is the stiffness matrix, pre-calculated analytically for uniform modulus using a boundary integral approach, w is the local natural fracture width, p is the local pressure and σ_N is the stress normal to the natural fracture face.